

# PCCP

Accepted Manuscript



This is an *Accepted Manuscript*, which has been through the Royal Society of Chemistry peer review process and has been accepted for publication.

*Accepted Manuscripts* are published online shortly after acceptance, before technical editing, formatting and proof reading. Using this free service, authors can make their results available to the community, in citable form, before we publish the edited article. We will replace this *Accepted Manuscript* with the edited and formatted *Advance Article* as soon as it is available.

You can find more information about *Accepted Manuscripts* in the [Information for Authors](#).

Please note that technical editing may introduce minor changes to the text and/or graphics, which may alter content. The journal's standard [Terms & Conditions](#) and the [Ethical guidelines](#) still apply. In no event shall the Royal Society of Chemistry be held responsible for any errors or omissions in this *Accepted Manuscript* or any consequences arising from the use of any information it contains.

Cite this: DOI: 10.1039/c0xx00000x

www.rsc.org/xxxxxx

ARTICLE TYPE

# Insights into the Mechanism of Oxidation of Dihydroorotate to Orotate Catalysed by Human Class 2 Dihydroorotate Dehydrogenase: A QM/MM Free Energy Study

Cláudio Nahum Alves,<sup>\*a,b</sup> José Rogério A. Silva<sup>a,b</sup> and Adrian E. Roitberg<sup>\*b</sup><sup>5</sup> Received (in XXX, XXX) Xth XXXXXXXXX 20XX, Accepted Xth XXXXXXXXX 20XX

DOI: 10.1039/b000000x

The Dihydroorotate Dehydrogenase (DHOD) enzyme catalyzes the unique redox reaction in the *de novo* pyrimidines biosynthesis pathway. In this reaction, the oxidation of dihydroorotate (DHO) to orotate (OA) and reduction of the flavin mononucleotide (FMN) cofactor is catalysed by DHOD. The class 2 DHOD, to which the human enzyme belongs, was experimentally shown to follow a stepwise mechanism but the data did not allow the determination of the order of bond-breaking in a stepwise oxidation of DHO. The goal of this study is to understand the reaction mechanism at molecular level of the class 2 DHOD, which may aid the design of inhibitors that selectively impact the activity of only certain members of the enzyme family. In this paper, the catalytic mechanism of oxidation of DHO to OA in human DHOD was studied using a hybrid Quantum Mechanical/Molecular Mechanical (QM/MM) approach and Molecular Dynamics (MD) simulations. The free energy barriers calculated reveal that the mechanism in human DHOD occurs via a stepwise reaction pathway. In the first step, a proton is abstracted from the C<sub>5</sub> of DHO to the deprotonated Ser215 side chain. Whereas, in the second step, the transfer of the hydride or hydride equivalent from the C<sub>6</sub> of DHO to the N<sub>5</sub> of FMN, where free energy barrier calculated by DFT/MM level is 10.84 kcal·mol<sup>-1</sup>. Finally, a residual decomposition analysis was carried out in order to elucidate the influence of the catalytic region residues during the DHO oxidation.

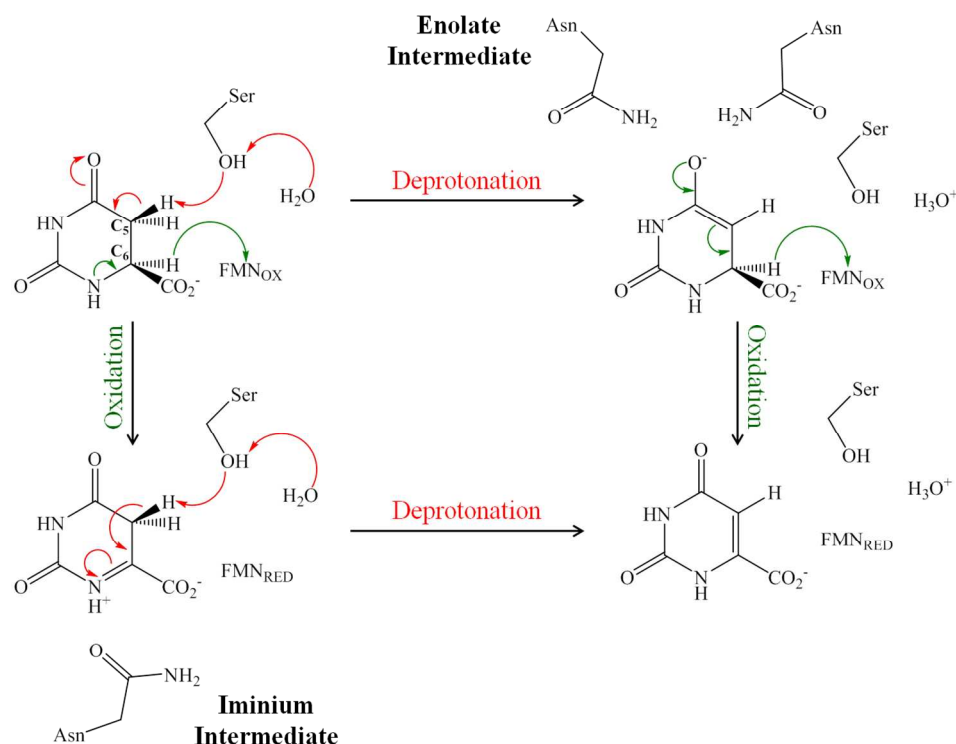
## Introduction

Dihydroorotate dehydrogenases (DHODs)<sup>1</sup> are flavin-containing enzymes that catalyze the fourth step in the *de novo* synthesis of pyrimidines. In this reaction, DHODs catalyze the conversion of dihydroorotate (DHO) to orotate (OA), the single redox step in pyrimidine synthesis. The diversity among DHODs of different organisms<sup>2</sup> could enable the development of compounds that selectively inhibit *de novo* pyrimidine biosynthesis in some organisms while not affecting others. Therefore, DHOD enzymes represent an attractive and selective target for treating cancer, malaria, gastric ulcers, and rheumatoid arthritis<sup>3-6</sup>. Many inhibitors have been developed to combat these diseases; some have been approved for use, as the case of the immunosuppressive drug leflunomide, which inhibits human DHOD and is used for the treatment of rheumatoid arthritis<sup>5,7,8</sup>.

DHODs can be classified into two classes based on sequence<sup>1</sup>: class 1 and class 2. Class 1 are cytoplasmic enzymes and can be further subdivided into subclasses 1A and 1B<sup>9,10</sup>. Class 1A enzymes (DHODs) form homodimers and appear to utilize Fumarate (FUM) as a physiological oxidant, in conjunction with oxidation of the reduced Flavin mononucleotide (FMN) cofactor during the second half-reaction<sup>10</sup>. Family 1B forms heterotetramers and utilize NAD<sup>+</sup> via a distinct protein subunit that contains a 2Fe–2S cluster and a Flavin Adenine dinucleotide

(FAD) cofactor<sup>9</sup>. Class 2 can be either homodimers or monomers and are membrane-bound enzymes that utilize respiratory quinone as a physiological oxidant during the second half-reaction<sup>11</sup>.

The mechanism of the dehydrogenation of dihydroorotic acid by DHOD has been the subject of extensive studies<sup>2,9,10,12-20</sup>. The oxidation reaction of DHO breaks two carbon-hydrogen bonds. An active site base (serine in class 2 enzymes or cysteine in class 1 enzymes) deprotonates C<sub>5</sub> of DHO, and a hydride (or hydrid equivalent) is transferred from C<sub>6</sub> of DHO to N<sub>5</sub> of the isoalloxazine ring of the flavin. The class 1 DHODs was demonstrated to follow a concerted mechanism<sup>13,17</sup>. On the other hand, the studies by Fagan and coworkers, using DHO deuterated at the 5-, 6-, and both positions in anaerobic stopped-flow experiments, indicated that the class 2 enzyme from *E. coli* and *H. sapiens* use a stepwise mechanism<sup>16,18</sup>. They suggested that when a stepwise mechanism occurs, there are two possible intermediates that could form: (i) if deprotonation occurs first, then an enolate intermediate will form, (ii) if hydride transfer occurs first, then an iminium intermediate will form (Scheme 1). It was not clear, in that study, which intermediate was forming in the stepwise oxidation of DHO by the class 2 DHOD enzymes.



**Scheme 1** The proposed mechanisms for the DHO oxidation by human DHOD enzyme.

We present a computational free energy study aimed to elucidate which intermediate is formed in human DHOD a class 2 of DHOD enzymes. Here, a hybrid Quantum Mechanics/Molecular Mechanics (QM/MM) approach and Molecular Dynamic (MD) simulations is applied to study the details of the catalytic mechanism of DHO oxidation in the class 2. Hybrid QM/MM approaches combined with MD simulations, have been employed for many studies involving protein-inhibitors interaction and catalytic mechanism enzymatic<sup>21-30</sup>. In the QM/MM methodology, one part of the system is described by quantum mechanics and the rest by molecular mechanics using a classical force field<sup>21, 29, 31</sup>. In this study, the density functional tight binding (DFTB) semiempirical method to describe the QM region of the system. The DFTB method not only has been shown to be an accurate level of theory for describing the energetic of chemical reactions<sup>32</sup>, but it was also demonstrated in biological systems that the minimum energy path results are in good agreement with higher levels of theory like MP2<sup>33</sup>. A previous theoretical study also shown that DFTB method provides the best semiempirical description of six-membered carbohydrate ring deformation<sup>34</sup>. Besides, recently, this semiempirical method was successfully applied to perform the catalytic mechanism for the DHOD from *L. lactis*<sup>35</sup>, a class 2 DHOD enzyme. An umbrella sampling method using an adequate reaction coordinate was employed in order to obtain the free energy profile associated with the catalytic mechanism of DHO oxidation by human DHOD. In addition, a detailed analysis of the stabilization pattern of the active site residues on the intermediate (IT) and transition state (TS), in relation to the Michaelis Complex (MC), is examined through of energy decomposition methods.

## Materials and methods

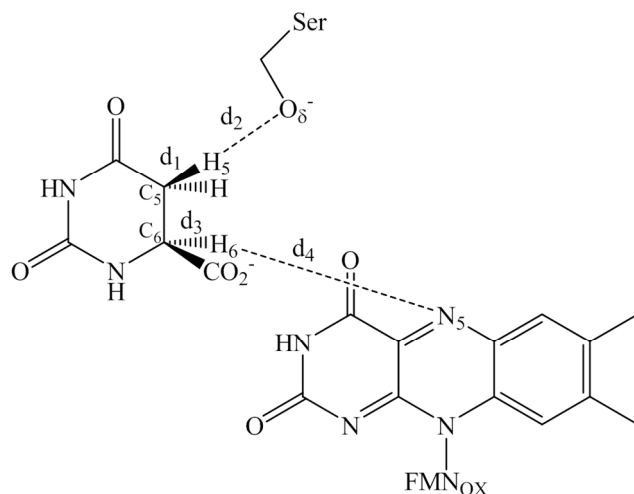
### Initial system aspects and QM/MM simulations

The initial coordinates of human DHOD were obtained from the PDB database (access code: 1D3G, resolved at 1.60 Å<sup>11</sup>). The human DHOD complex consist of 313 amino acid residues, 248 crystalline water molecules and the OA product and FMN cofactor bound in active site. In our simulations, the OA was “mutated”, *in silico*, to the DHO substrate. The missing hydrogen atoms were added to the system using the Leap module of Amber12 package<sup>36</sup> taking into account a previous assignment of the protonation states of all these residues at pH 7 performed by recalculating the standard pKa values of the titratable amino acids using the empirical *propKa* program of Jensen *et al*<sup>37</sup>. Particularly, the catalytic residue Ser215 was already considered in its active state (deprotonated), in accordance with experimental kinetics data<sup>38</sup>. The system was immersed in a truncated octahedral cell of TIP3P<sup>39</sup> water molecules, extending 10 Å outside the protein on each side. The force field parameters for the protein were assigned from the *ff99SB*<sup>40</sup>, while the DHO substrate were obtained from *gaff*<sup>41</sup>. The RESP approach was applied to obtain the substrate charges using HF/6-31G\* level of theory calculated in Gaussian09 program<sup>42</sup>. The FMN cofactor<sup>43</sup> was described using parameter sets available in Bryce Group website.

The initial complex prepared as described on the previous paragraph were first submitted to 10000 steps of conjugate gradient energy minimization using the sander module of Amber12 package. Then, the complex was energy-minimized and then gradually heated to 300 K over 2 ns with a harmonic constraint value of 10 kcal·mol<sup>-1</sup>·Å<sup>-2</sup> applied to the solute. Finally, the heated complex was equilibrated for 200 ps before the production stage. The minimizations, heating, equilibration and production stages employed a non-bonded cut-off of 8 Å. The particle mesh Ewald (PME) approach was applied to

calculate the long-range Coulomb Forces. The time step was set to 2 fs and all bonds involving hydrogen atoms were constrained using the SHAKE algorithm<sup>44</sup> during the MD simulation.

For the hybrid QM/MM simulations with DHOD-DHO complex, the atoms of the DHO, FMN and side chain of the deprotonated Ser215 amino acid residue were selected for QM region, which contains 49 atoms. The self-consistent charge density functional tight binding (scc-DFTB) semiempirical method<sup>45</sup>, as implemented in Amber12<sup>46</sup>, was selected to describe the QM region, while MM region of the complex (protein and water molecules) was described using the *ff99SB*<sup>40</sup> and TIP3P<sup>39</sup> parameter sets, respectively, as described early. The link atom method was used<sup>47</sup> to complete the valence of the QM fragments into the QM-MM boundary in all part of QM system.



**Scheme 2** Representation of the reaction coordinates used to elucidate the DHO oxidation by human DHOD.

### Umbrella Sampling and 2D Free Energy Surface (2D-FES)

The equilibrated structure was used as the initial point for the Umbrella Sampling simulations. The distances involved in the reaction coordinate definitions are described in Scheme 2:  $d_1$  refers to the distance between the C<sub>5</sub> and H<sub>5</sub> atoms from the substrate DHO, and  $d_2$  is the distance between the H<sub>5</sub> atom of DHO and the O<sub>γ</sub> atom of catalytic residue Ser215.  $d_3$  defines the distance between C<sub>6</sub> and H<sub>6</sub> atoms from the substrate DHO while  $d_4$  describes the distance between H<sub>6</sub> atom of DHO and the N<sub>5</sub> atom of FMN cofactor. The proton abstraction step (RC1) is described by the distances combination  $d_1-d_2$  while the hydride transfer step (RC2) is described by the distances combination  $d_3-d_4$ . A 2D-FES was evaluated in order to explore the oxidation of DHO in the mechanism of human DHOD enzyme using RC1 versus RC2. RC1 was sampled from -0.40 to 1.40 Å while RC2 was scanned from -1.00 to 1.60 Å. The umbrella were spaced in steps of 0.10 Å. In each window, 10 ps of production were preceded by 5 ps of equilibration, with a time step of 0.5 fs. All QM/MM MD simulations were performed constraining the value of the two RCs with harmonic potential using a force constant of 200.0 kcal·mol<sup>-1</sup>·Å<sup>-2</sup>. The 2D weighted histogram analysis method (WHAM-2D)<sup>48</sup> implemented in the package written by Alan Grossfield<sup>49</sup> was used to obtain the potentials of mean force (PMF) profile for the unbiased system along the reaction coordinates. Finally, the PMFs were corrected by means of

B3LYP-D3/MM and MP2/MM single-point energies for the reaction path (see ESI for details).

45

### Interaction Energy Decomposition

In order to analyze how the active site residues stabilize/destabilize the INT and TS states in the catalyzed reaction of DHO by human DHOD with respect to MC state, we performed an energy decomposition analysis. This type of analysis has been extensively applied to enzymatic systems<sup>24, 50-56</sup>. As the method has been discussed in detail elsewhere, here, just the main equations are presented.

The influence of a particular residue on the energy of a determined ensemble state is measured taking into account the difference of energies when an individual residue is present (named by  $i$  in eq 1) or when it is mutated to Gly ( $i-1$  in eq 1)<sup>57, 58</sup>.

$$\Delta E_i = [E_i^{\text{QM}} + E_i^{\text{QM/MM}}] - [E_{i-1}^{\text{QM}} + E_{i-1}^{\text{QM/MM}}] \quad (1)$$

where each term in brackets means the energy of the QM part influenced by the classical environment. Then, the differences between the stabilization effects in going from MC to INT (or TS), for each residue, were estimated by

$$\Delta \Delta E_i = \Delta E_i^{\text{INT/TS}} - \Delta E_i^{\text{MC}} \quad (2)$$

In our analysis, the QM subsystem was composed of the substrate, cofactor and Ser215. To obtain the average values for the interaction energy and stabilization effects of each residue in a particular state, 400 snapshots from QM/MM MD simulations were considered taken from umbrella sampling calculation with reaction coordinates corresponding to the MC, INT and TS. As no MD simulation is run when the  $i$ -th residue is mutated to Gly, the  $\Delta \Delta E_i$  does not consider the dynamic effects arising from differences in the structure/dynamics of the enzyme upon replacement. The  $\langle \Delta \Delta E_i \rangle$  values provide hints about detrimental/beneficial effects of the  $i$ th residue for the mechanism step under observation. Finally, these values cannot be considered to quantitatively estimate changes in the catalytic constant produced by mutation of the  $i$ -th residue by Gly for such changes depend on variations in the activation free energy,  $\Delta G^\ddagger$ .

## Results and discussion

In the crystal structures of class 2 DHODs, residue Ser215 has been identified as the catalytic base, with one water molecule forming a bridge between Ser215 and Thr218 residues<sup>11</sup>. In this enzyme, Ser215 is not exposed to solvent but a hydrogen bond network connects the active site base to bulk solvent. Small and coworkers<sup>59</sup> using MD found the same hydrogen bond network which was observed experimentally. In that study, a proton relay mechanism had been hypothesized to facilitate the proton-transfer reaction from substrate to Ser215. In this sense, the proton would be passed from C<sub>5</sub> of DHO to the active site Ser215 to the water molecule in the tunnel, to a conserved Thr residue, and finally to bulk solvent, i.e., this network shuttles protons from the active site to bulk solvent and, therefore, could have a role in allowing the serine to act as a base<sup>38, 59</sup>. Fagan and co-workers through experimental evidences suggest a deprotonated state for the catalytic Ser residue<sup>16</sup>. Besides, a recent computational study for the DHOD from *L. lactis* started the catalytic base (Cys residue) for the mechanism already in its deprotonated state<sup>35</sup>. Moreover, DHOD enzymes from Class 1A have their active sites much more

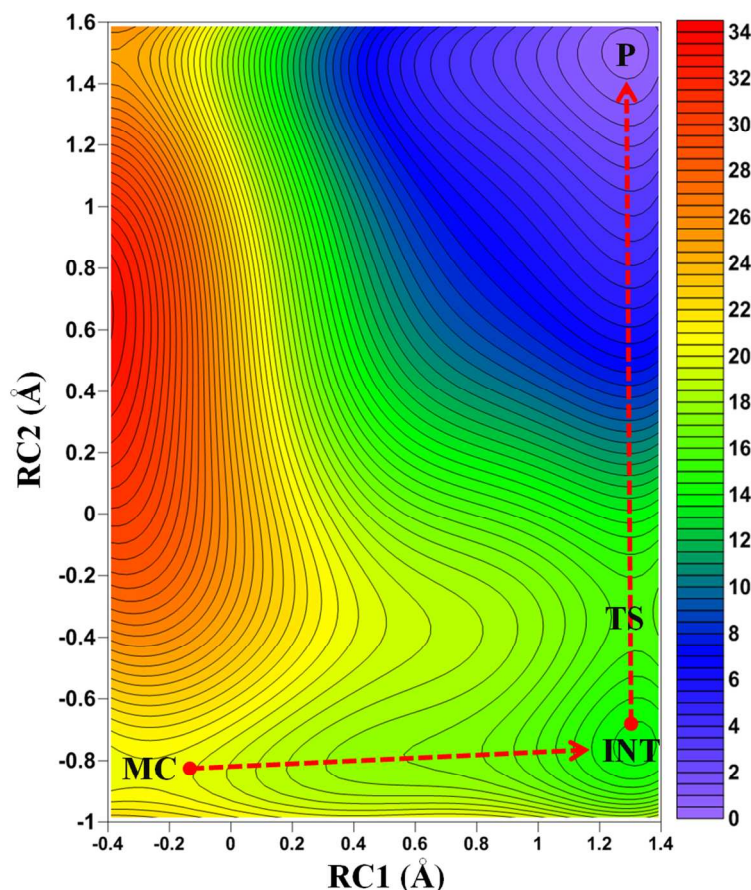


Fig. 1 2D plot of FES for the DHO oxidation in human DHOD obtained by umbrella sampling simulations. The energy values are reported in kcal·mol<sup>-1</sup>

exposed to solvent than Class 2. Then, in these enzymes (Class 2), just an active serine alone is not enough; in this way, a fully proton relay network should be ordered for the most effective DHO deprotonation<sup>38</sup>. Therefore, in our study the catalytic Ser215 residue was already considered in its deprotonated form given previous experimental and theoretical data<sup>11, 16, 18, 38, 59</sup>.

#### Umbrella Sampling and 2D-FES

In order to investigate the molecular mechanism of the oxidation of DHO to OA in human DHOD, we have employed umbrella sampling using DFTB/MM level. Figure 1 depicts the 2D-FES obtained through the RC1 versus RC2 described in the previous section. The changes in the distances involved in the reaction coordinate definition, as well as averaged geometrical parameters for MC, INT, TS and P structures are presented in Table 1. As shown in Figure 1 and Table 1, the mechanism in human DHOD occurs via a stepwise reaction pathway. Importantly, this result supports the stepwise mechanism found experimentally for class 2 enzyme from *E. coli* and *H. sapiens*<sup>16, 18</sup>. The first step of the molecular mechanism is the proton is abstracted from C<sub>5</sub> of DHO to deprotonated Ser215 side chain, and, the enolate intermediate is generated. In the second step the hydride or hydride equivalent is abstracted from C<sub>6</sub> of DHO to N<sub>5</sub> of FMN, completing the oxidation of the DHO into OA.

**Table 1** Average distances collected from QM/MM MD simulations of reaction chemical species. The standard deviation values are present in parenthesis

DFTB/MM	MC	INT	TS	P
$d(\text{C}_5\text{-H}_5)$	1.25 (0.03)	2.30 (0.04)	2.30 (0.04)	2.29 (0.04)
$d(\text{H}_5\text{-O}_\delta)$	1.55 (0.04)	0.99 (0.02)	0.99 (0.03)	0.99 (0.03)
$d(\text{C}_6\text{-H}_6)$	1.16 (0.04)	1.16 (0.03)	1.28 (0.04)	2.52 (0.04)
$d(\text{H}_6\text{-N}_5)$	2.06 (0.04)	1.95 (0.04)	1.58 (0.04)	1.02 (0.03)

In the first step (proton abstraction step), the  $d_1$  bond distance changes from 1.25 Å in MC to 2.30 Å in INT, while the  $d_2$  distance changes from 1.55 Å in MC to 0.99 Å in INT, showing that proton transfer takes place before the hydride transference. Interestingly, during the proton abstraction step the transition state was not identified; an experimental kinetic isotope effects study for the class 2 enzyme from *E. coli* show the deprotonation of C5 atom of DHO is fast enough that it does not contribute in the kinetic of the reaction<sup>16</sup>. The computed  $\Delta G^\circ$  for this step is  $-6.54$  kcal·mol<sup>-1</sup> making the INT more stable than MC, which agrees with previous experimental analyzes<sup>16</sup>. In the second transfer of the hydride or hydride equivalent step, the  $d_3$  bond distance increases from 1.16 Å in INT to 1.28 Å in transition state (TS1) and then to 2.52 Å in P, while the  $d_4$  distance changes from

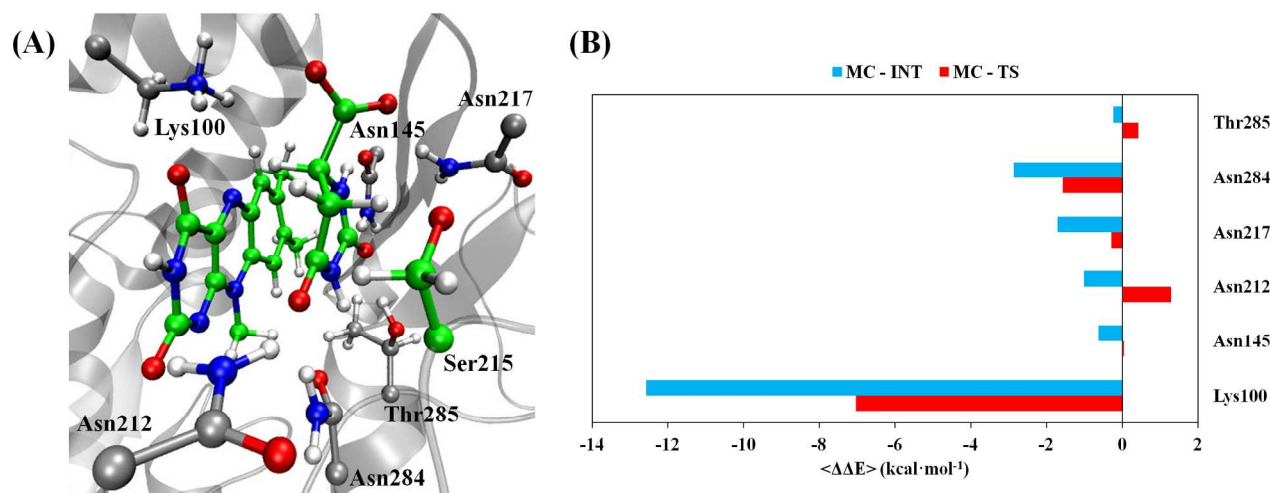


**Fig. 2** (A) The representative MC frame on 2D-FES considered on the residual decomposition analysis. The QM subsystem is presented on green carbon atoms. (B) Plot of stabilization of the TS (red) and INT (blue) states with respect to the MC by active region residues.

1.95 Å in INT to 1.58 Å in TS1 and then to 1.02 Å in P, indicating the transference of the hydride from C<sub>6</sub> of DHO to N<sub>5</sub> of FMN takes place after the proton abstraction step. On this step, the computed  $\Delta G^\circ$  is  $-13.50 \text{ kcal}\cdot\text{mol}^{-1}$  making the transfer of the hydride thermodynamically favourable.

The free energy barrier ( $\Delta G^\ddagger$ ) obtained by DFTB/MM level, between INT and P is  $2.04 \text{ kcal}\cdot\text{mol}^{-1}$  ( $10.84$  and  $7.55 \text{ kcal}\cdot\text{mol}^{-1}$  using B3LYP-D3/MM and MP2/MM corrections, respectively) for the hydride equivalent step. This result rationalize the experimental evidence that identifies DHOD as a very fast enzyme (fast enough that the experimental procedures must be carried out at low temperatures to be measurable) and suggests that DHO oxidation occurs via a stepwise mechanism for DHOD class 2 enzymes, which is in agreement with mechanisms proposed by Fagan and coworkers<sup>16</sup>.

Finally, in order to evaluate the mechanism found at DFTB/MM level, we also performed B3LYP-D3/MM and MP2/MM calculations. In this calculation, we carried out single-point calculations using representative snapshots from MC, INT, TS and P states. It confirms that the proton abstraction step is kinetic and thermodynamically followed by the hydride equivalent step (see supplementary data).

### Interaction Energy Decomposition

The origin of the substrate-enzyme interaction can be analyzed by decomposing the total interaction energy and taking into account the difference of energies when a particular residue is present, as described in the method section. In order to get a deep insight into protein-substrate interactions, 400 snapshots from QM/MM MD simulations were considered taken from umbrella sampling calculation, for substrate-protein complexes appearing along the 2D-FES (MC, INT and TS). Figure 2a shows how the main amino acid residues interact in the active site. Averaged protein-substrate interaction energies by residue in MC and relative stabilization pattern on the INT and TS with respect to the MC are displayed in Figure 2b. The addition over all the  $\Delta \Delta E$  values for each residue represents an indication of the degree of the stabilization of the INT and TS from the enzyme environment on

the QM subsystem. The resultant values were  $-19.03$  and  $-7.12 \text{ kcal}\cdot\text{mol}^{-1}$ , indicating a strong stabilizing effect on the INT and TS, respectively. From Figure 2a we can observe how the MC interacts through hydrogen bonds, with a pocket created by Lys100, Asn145, Asn212, Asn217, Asn284 and Thr285 residues. The Asn145, Asn212, Asn217, Asn284 and Thr285 residues are conserved in all DHODs sequences<sup>2, 11, 60-65</sup>. Lys100, which is conserved in family 2 members, also form also hydrogen bond with FMN. The specific function of each residue during the DHO oxidation mechanism is still unknown<sup>18</sup>. They would play a role in the conversion of the DHO into OA by stabilizing the chemical species found during the catalytic mechanism, i.e., the transition state and/or the intermediate, as well as the binding of DHO for the reaction. Then, in order to elucidate and to try better understanding their roles, an interaction energy decomposition analysis was computed. In Figure 2b, positive values correspond to unfavorable interactions, whereas negative values mean that the interaction is stabilizing the substrate in that particular state.

The Figure 2b shows the relative stabilization pattern on the INT and TS with respect to the MC. The INT enzyme complex presents a stabilization pattern stronger to the one observed for TS enzyme. Thus, our analysis will be focused on the INT and TS. A detailed analysis of the stabilization pattern residues to the total INT complex and TS complex stabilization energy shows that while the strongest interaction of INT is established with the Lys100, Asn145, Asn212, Asn217, Asn284 and Thr285 residues, while in the case of TS2, it is with just Lys100, Asn217 and Asn284 residues. The Asn212 and Asn284 are well positioned to stabilize any partial negative charge that developed at the DHO in INT, and, therefore, it stabilizes the formation of enolate intermediate, while Asn154 does not show an important role during stabilizing any chemical species, once that iminium intermediate is not created during the DHO oxidation. Therefore, these results evidence the formation of enolate as the reaction intermediate. In fact, Fagan and co-workers demonstrated that the mutation of Asn212 and Asn284 results in a large decrease in the reduction rate constant ( $10500$ -fold and  $2000$ -fold, respectively), i.e., the Asn212 and Asn284 residues are important for catalytic

mechanism performance. These findings are also in agreement with our previous QM/MM studies of the mechanism of class 1A DHOD from *Trypanosoma cruzi*<sup>19</sup>.

## Conclusions

We have investigated the mechanism of the catalytic mechanism of oxidation of DHO to OA in human DHOD through DFTB/MM MD calculations. The results obtained show that the mechanism in human DHOD occurs via a stepwise reaction pathway. In the first step of the molecular mechanism the proton is abstracted from C<sub>5</sub> of DHO to deprotonated Ser215 side chain, and, in the second step the transfer of the hydride or hydride equivalent from C<sub>6</sub> of DHO to N<sub>5</sub> of FMN occurs. The  $\Delta G^\ddagger$  obtained for the reaction by DFTB/MM level is 2.04 kcal·mol<sup>-1</sup> for second step; however, by means B3LYP-D3/MM and MP2/MM single point calculations, the  $\Delta G^\ddagger$  value increase to 10.84 and 7.55 kcal·mol<sup>-1</sup>, respectively, which is suitable to experimental evidences. As observed in the analysis of individual interactions, the influence of Lys100, Asn212 and Asn284 seems to be crucial for FMN reduction. Thus, the present theoretical study is not only important to get an insight into the reaction, but the knowledge of the molecular mechanism can be used to get structural and electronic information of the species appearing along an enzymatic reaction path, which is of great value for a systematic protocol for synthesis of inhibitors. We hope it can contribute to future studies of this important system and could eventually facilitate development of the inhibitors for treating cancer, malaria, gastric ulcers, and rheumatoid arthritis.

## Acknowledgments

We thank financial support from Conselho Nacional de Desenvolvimento Científico e Tecnológico (CNPq), Pró-Reitoria de Pesquisa de Pós-Graduação da Universidade Federal do Pará (PROPEP-UFPA). Alves, C. N. and Silva, J.R.A. thank Coordenação de Aperfeiçoamento de Pessoal de Nível Superior (CAPES) for financial support. The authors acknowledge the University of Florida Research Computing for providing computational resources and support that have contributed to the research results reported in this publication. We also thank Justin Smith for the corrections and suggestions in English writing that help to improve this study.

## Notes

<sup>a</sup> Laboratório de Planejamento e Desenvolvimento de Fármacos, Instituto de Ciências Exatas e Naturais, Universidade Federal do Pará, Belém, Brazil. Fax: 55 91-3201-7633; Tel: 55 91-3201-8235; E-mail: nahum@ufpa.br

<sup>b</sup> Department of Chemistry, University of Florida, Gainesville, Florida, United States. Fax: 352 392-8722; Tel: 352 392-6972; E-mail: roitberg@ufl.edu

† Electronic Supplementary Information (ESI) available: [details of the free energy barrier correction to the SCC-DFTB/MM by B3LYP-D3/MM and MP2/MM]. See DOI: 10.1039/b000000x/

## References

- O. Bjornberg, P. Rowland, S. Larsen and K. F. Jensen, *Biochemistry*, 1997, 36, 16197-16205.
- P. Rowland, O. Bjornberg, F. S. Nielsen, K. F. Jensen and S. Larsen, *Protein Science*, 1998, 7, 1269-1279.
- G. Weber, *Cancer Research*, 1983, 43, 3466-3492.
- W. L. Elliott, D. P. Sawick, S. A. Defrees, P. F. Heinstein, J. M. Cassady and D. J. Morre, *Biochimica Et Biophysica Acta*, 1984, 800, 194-201.
- F. C. Breedveld and J. M. Dayer, *Annals of the Rheumatic Diseases*, 2000, 59, 841-849.
- B. A. Palfey, O. Bjornberg and F. Jensen, *Journal of Medicinal Chemistry*, 2001, 44, 2861-2864.
- H. M. Cherwinski, N. Byars, S. J. Ballaron, G. M. Nakano, J. M. Young and J. T. Ransom, *Inflammation Research*, 1995, 44, 317-322.
- H. M. Cherwinski, R. G. Cohn, P. Cheung, D. J. Webster, Y. Z. Xu, J. P. Caulfield, J. M. Young, G. Nakano and J. T. Ransom, *Journal of Pharmacology and Experimental Therapeutics*, 1995, 275, 1043-1049.
- F. S. Nielsen, P. Rowland, S. Larsen and K. F. Jensen, *Protein Science*, 1996, 5, 852-856.
- M. Nagy, F. Lacroute and D. Thomas, *Proceedings of the National Academy of Sciences of the United States of America*, 1992, 89, 8966-8970.
- S. P. Liu, E. A. Neidhardt, T. H. Grossman, T. Ocain and J. Clardy, *Structure with Folding & Design*, 2000, 8, 25-33.
- P. Rowland, F. S. Nielsen, K. F. Jensen and S. Larsen, *Structure*, 1997, 5, 239-252.
- R. L. Fagan, K. F. Jensen, O. Bjornberg and B. A. Palfey, *Biochemistry*, 2007, 46, 4028-4036.
- O. Bjornberg, D. B. Jordan, B. A. Palfey and K. F. Jensen, *Archives of Biochemistry and Biophysics*, 2001, 391, 286-294.
- S. Norager, S. Arent, O. Bjornberg, M. Ottosen, L. Lo Leggio, K. F. Jensen and S. Larsen, *Journal of Biological Chemistry*, 2003, 278, 28812-28822.
- R. L. Fagan, M. N. Nelson, P. M. Pagano and B. A. Palfey, *Biochemistry*, 2006, 45, 14926-14932.
- P. Rowland, S. Norager, K. F. Jensen and S. Larsen, *Structure*, 2000, 8, 1227-1238.
- R. L. Fagan and B. A. Palfey, *Biochemistry*, 2009, 48, 7169-7178.
- N. d. F. Silva, J. Lameira, C. N. Alves and S. Marti, *Physical Chemistry Chemical Physics*, 2013, 15, 18863-18871.
- H. Munier-Lehmann, P.-O. Vidalain, F. Tanguy and Y. L. Janin, *Journal of Medicinal Chemistry*, 2013, 56, 3148-3167.
- A. Warshel and M. Levitt, *Journal of Molecular Biology*, 1976, 103, 227-249.
- S. Marti, J. Andres, V. Moliner, E. Silla, I. Tunon and J. Bertran, *Chemical Society Reviews*, 2008, 37, 2634-2643.
- J. J. Ruiz-Pernia, E. Silla, I. Tunon and S. Marti, *Journal of Physical Chemistry B*, 2006, 110, 17663-17670.
- G. Pierdominici-Sottile, N. A. Horenstein and A. E. Roitberg, *Biochemistry*, 2011, 50, 10150-10158.
- M. Reis, C. N. Alves, J. Lameira, I. Tunon, S. Marti and V. Moliner, *Physical Chemistry Chemical Physics*, 2013, 15, 3772-3785.

26. M. W. van der Kamp and A. J. Mulholland, *Biochemistry*, 2013, 52, 2708-2728.
27. H. M. Senn and W. Thiel, *Angewandte Chemie-International Edition*, 2009, 48, 1198-1229.
28. M. J. Field, M. Albe, C. Bret, F. Proust-De Martin and A. Thomas, *Journal of Computational Chemistry*, 2000, 21, 1088-1100.
29. E. Rosta, M. Klahn and A. Warshel, *Journal of Physical Chemistry B*, 2006, 110, 2934-2941.
30. C. N. Alves, S. Marti, R. Castillo, J. Andres, V. Moliner, I. Tunon and E. Silla, *Biophys J*, 2008, 94, 2443-2451.
31. A. Warshel, *Annual Review of Biophysics and Biomolecular Structure*, 2003, 32, 425-443.
32. T. Kruger, M. Elstner, P. Schifffels and T. Frauenheim, *Journal of Chemical Physics*, 2005, 122.
33. H. L. Woodcock, M. Hodoscek and B. R. Brooks, *Journal of Physical Chemistry A*, 2007, 111, 5720-5728.
34. C. B. Barnett and K. J. Naidoo, *Journal of Physical Chemistry B*, 2010, 114, 17142-17154.
35. J. R. A. Silva, A. E. Roitberg and C. N. Alves, *Journal of Physical Chemistry B*, 2015, 119, 1468-1473.
36. D. Case, T. A. Darden, T. E. Cheatham, C. Simmerling, J. Wang, R. Duke, R. Luo, M. Crowley, R. Walker, W. Zhang, K. M. Merz, B. Wang, S. Hayik, A. Roitberg, G. Seabra, I. Kolossváry, K. F. Wong, F. Paesani, J. Vanicek, X. Wu, S. Brozell, T. Steinbrecher, H. Gohlke, L. Yang, C. Tan, J. Mongan, V. Hornak, G. Cui, D. H. Mathews, M. G. Seetin, C. Sagui, V. Babin and P. Kollman, *AMBER 12*, University of California, San Francisco, 2012.
37. H. Li, A. D. Robertson and J. H. Jensen, *Proteins-Structure Function and Bioinformatics*, 2005, 61, 704-721.
38. R. L. Kow, J. R. Whicher, C. A. McDonald, B. A. Palfey and R. L. Fagan, *Biochemistry*, 2009, 48, 9801-9809.
39. W. L. Jorgensen, J. Chandrasekhar, J. D. Madura, R. W. Impey and M. L. Klein, *Journal of Chemical Physics*, 1983, 79, 926-935.
40. V. Hornak, R. Abel, A. Okur, B. Strockbine, A. Roitberg and C. Simmerling, *Proteins-Structure Function and Bioinformatics*, 2006, 65, 712-725.
41. J. M. Wang, R. M. Wolf, J. W. Caldwell, P. A. Kollman and D. A. Case, *Journal of Computational Chemistry*, 2004, 25, 1157-1174.
42. M. J. Frisch, G. W. Trucks, H. B. Schlegel, G. E. Scuseria, M. A. Robb, J. R. Cheeseman, G. Scalmani, V. Barone, B. Mennucci, G. A. Petersson, H. Nakatsuji, M. Caricato, X. Li, H. P. Hratchian, A. F. Izmaylov, J. Bloino, G. Zheng, J. L. Sonnenberg, M. Hada, M. Ehara, K. Toyota, R. Fukuda, J. Hasegawa, M. Ishida, T. Nakajima, Y. Honda, O. Kitao, H. Nakai, T. Vreven, J. A. Montgomery, J. E. Peralta, F. Ogliaro, M. Bearpark, J. J. Heyd, E. Brothers, K. N. Kudin, V. N. Staroverov, R. Kobayashi, J. Normand, K. Raghavachari, A. Rendell, J. C. Burant, S. S. Iyengar, J. Tomasi, M. Cossi, N. Rega, J. M. Millam, M. Klene, J. E. Knox, J. B. Cross, V. Bakken, C. Adamo, J. Jaramillo, R. Gomperts, R. E. Stratmann, O. Yazyev, A. J. Austin, R. Cammi, C. Pomelli, J. W. Ochterski, R. L. Martin, K. Morokuma, V. G. Zakrzewski, G. A. Voth, P. Salvador, J. J. Dannenberg, S. Dapprich, A. D. Daniels, Farkas, J. B. Foresman, J. V. Ortiz, J. Cioslowski and D. J. Fox, Wallingford CT, 2009, DOI: citeulike-article-id:9096580.
- C. Schneider and J. Suhnel, *Biopolymers*, 1999, 50, 287-302.
- J. P. Ryckaert, G. Ciccotti and H. J. C. Berendsen, *Journal of Computational Physics*, 1977, 23, 327-341.
- M. Elstner, D. Porezag, G. Jungnickel, J. Elsner, M. Haugk, T. Frauenheim, S. Suhai and G. Seifert, *Physical Review B*, 1998, 58, 7260-7268.
- G. d. M. Seabra, R. C. Walker, M. Elstner, D. A. Case and A. E. Roitberg, *Journal of Physical Chemistry A*, 2007, 111, 5655-5664.
- M. J. Field, P. A. Bash and M. Karplus, *Journal of Computational Chemistry*, 1990, 11, 700-733.
- S. Kumar, D. Bouzida, R. H. Swendsen, P. A. Kollman and J. M. Rosenberg, *Journal of Computational Chemistry*, 1992, 13, 1011-1021.
- S. Grossfield, WHAM: the weighted histogram analysis method, version 2.0.9, <http://membrane.urmc.rochester.edu/content/wham>.
- D. C. Chatfield, K. P. Eurenium and B. R. Brooks, *Theochem-Journal of Molecular Structure*, 1998, 423, 79-92.
- A. R. Dinner, G. M. Blackburn and M. Karplus, *Nature*, 2001, 413, 752-755.
- M. Garcia-Viloca, D. G. Truhlar and J. L. Gao, *Biochemistry*, 2003, 42, 13558-13575.
- C. Hensen, J. C. Hermann, K. H. Nam, S. H. Ma, J. L. Gao and H. D. Holtje, *Journal of Medicinal Chemistry*, 2004, 47, 6673-6680.
- G. Pierdominici-Sottile and A. E. Roitberg, *Biochemistry*, 2011, 50, 836-842.
- J. R. A. Silva, A. E. Roitberg and C. N. Alves, *Journal of Chemical Information and Modeling*, 2014, 54, 2402-2410.
- G. Pierdominici-Sottile, R. Cossio Perez, J. F. Galindo and J. Palma, *Plos One*, 2014, 9.
- D. T. Major and J. Gao, *Journal of the American Chemical Society*, 2006, 128, 16345-16357.
- K.-Y. Wong and J. Gao, *Biochemistry*, 2007, 46, 13352-13369.
- Y. A. Small, V. Guallar, A. V. Soudackov and S. Hammes-Schiffer, *Journal of Physical Chemistry B*, 2006, 110, 19704-19710.
- S. Norager, K. F. Jensen, O. Bjornberg and S. Larsen, *Structure*, 2002, 10, 1211-1223.
- T. L. Arakaki, F. S. Buckner, J. R. Gillespie, N. A. Malmquist, M. A. Phillips, O. Kalyuzhnyi, J. R. Luft, G. T. DeTitta, C. L. M. J. Verlinde, W. C. Van Voorhis, W. G. J. Hol and E. A. Merritt, *Molecular Microbiology*, 2008, 68, 37-50.
- D. K. Inaoka, K. Sakamoto, H. Shimizu, T. Shiba, G. Kurisu, T. Nara, T. Aoki, K. Kita and S. Harada, *Biochemistry*, 2008, 47, 10881-10891.
- A. T. Cordeiro, P. R. Feliciano, M. P. Pinheiro and M. Cristina Nonato, *Biochimie*, 2012, 94, 1739-1748.
- J. Cheleski, J. R. Rocha, M. P. Pinheiro, H. J. Wiggers, A. B. F. da Silva, M. C. Nonato and C. A. Montanari, *European Journal of Medicinal Chemistry*, 2010, 45, 5899-5909.

- 
65. J. Cheleski, H. J. Wiggers, A. P. Citadini, A. J. da Costa Filho, M. C. Nonato and C. A. Montanari, *Analytical Biochemistry*, 2010, 399, 13-22.